THERAPEUTIC EFFECTS OF HYPOXIC AND PRO-INFLAMMATORY PRIMING OF MESENCHYMAL STEM CELL-DERIVED EXTRACELLULAR VESICLES IN INFLAMMATORY ARTHRITIS

Alasdair G. Kay[1], Kane Treadwell[2], Paul Roach[3], Rebecca Morgan[2], Rhys Lodge[4], Mairead Hyland[2], Anna M.Piccinini[5], Nicholas Forsyth[6], *Oksana Kehoe[2]

[1]Department of Biology, University of York, York, UK; [2]School of Medicine, Keele University at the RJAH Orthopaedic Hospital, Oswestry, UK; [3]Chemistry Department, Loughborough University, Loughborough, UK; [4]School of Chemistry, University of Nottingham, Nottingham, UK; [5]School of Pharmacy, University of Nottingham, Nottingham, UK; [6]School of Pharmacy and Bioengineering, Keele University, The Guy Hilton Research Laboratories, Hartshill, Stoke on Trent, UK

*Correspondence and requests for materials should be addressed to O.K. (email: o.kehoe@keele.ac.uk)

Abstract

Novel biological therapies have revolutionised the management of Rheumatoid Arthritis (RA) but no cure currently exists. Mesenchymal stem cells (MSCs) immunomodulate inflammatory responses through paracrine signalling, including via secretion of extracellular vesicles (EVs) in the cell secretome. We evaluated the therapeutic potential of MSCs-derived small EVs in an antigen-induced model of arthritis (AIA).

EVs isolated from MSCs cultured normoxically (21% O_2, 5% CO_2), hypoxically (2% O_2, 5% CO_2) or with a pro-inflammatory cytokine cocktail were applied into the AIA model. Disease pathology was assessed post-arthritis induction through swelling and histopathological analysis of synovial joint structure. Activated CD4+ T cells from healthy mice were cultured with EVs or MSCs to assess deactivation capabilities prior to application of standard EVs in vivo to assess T cell polarisation within the immune response to AIA.

All EVs treatments reduced knee-joint swelling whilst only normoxic and pro-inflammatory primed EVs improved histopathological outcomes. In vitro culture with EVs did not achieve T cell deactivation. Polarisation towards CD4+ helper cells expressing IL17a (Th17) was reduced when normoxic and hypoxic EV treatments were applied in vitro. Normoxic EVs applied into the AIA model reduced Th17 polarisation and improved Th17:Treg homeostatic balance.

Priming of MSCs in EV production can be applied to alter the therapeutic efficacy however normoxic EVs present the optimal strategy for broad therapeutic benefit. The varied outcomes observed in MSCs priming may promote EVs optimised for therapies targeted for specific therapeutic priorities. EVs present an effective novel technology with potential for cell-free therapeutic translation.

Keywords

Rheumatoid Arthritis, inflammation, immunomodulation, extracellular vesicles, mesenchymal stem cells

Introduction

Mesenchymal stem cells (MSCs) are a promising therapeutic option owing potential for tissue repair through trilineage differentiation capacity, immunomodulatory properties disrupting T cell proliferation, B cell function and dendritic cell (DCs) maturation; and promoting anti-inflammatory responses mediated through macrophage interactions[1]. Widespread introduction of stem cell therapies has been hindered by inconsistent outcomes at clinical trial and donor variability. Our group has demonstrated the immunomodulatory capacity of both MSCs and their conditioned medium (CM-MSC) to reduce inflammation in a murine antigen-induced arthritis (AIA) model through enhanced Treg function and restored Treg:Th17 ratio[2,3]. MSCs convey their immunomodulatory properties through cell-to-cell contact, autocrine responses and paracrine signalling[1], including through secretion of . extracellular vesicles (EVs)[4]. EVs are membrane bound particles that carry a cargo of microRNA (miRNA), mRNA, lipid, carbohydrate and protein signals to facilitate intercellular communication[5-9]. Notably, disease severity in seropositive RA has been linked to EVs signalling[10-15]. MSC-derived EVs have been shown to be beneficial in autoimmune disorders in functioning to modulate autoimmune responses, particularly related to graft rejection and hypertension[16-18] but also in inflammatory arthritis and rheumatic diseases[19-21]. T cells have been shown to recruit EVs released by DCs, suggesting an integral action in orchestrating *in*

64 *vivo* immune responses[22,23]. Furthermore, tolerance in DCs is influenced by CD4+ T cells
65 through EVs-mediated intercellular signalling mediated by transfer of EVs-packaged miRNA[24].

66 We hypothesised that EVs recapitulate the anti-inflammatory and immunomodulatory effects
67 of MSCs in the arthritis model and that priming MSCs during the generation of EVs through
68 hypoxic culture or pro-inflammatory cytokine cocktails will enhance therapeutic outcomes.

69 Identification of the most effective cell source and maintenance conditions for generation of
70 optimally efficacious EVs will accelerate development of EV therapeutics for RA and other
71 regenerative medicine targets. To date, no research has directly examined and contrasted the
72 influence of cell isolation and priming on EVs generation using both hypoxia and pro-
73 inflammatory pre-conditioning of MSCs during production.

74 Here we present novel data utilising priming strategies for MSC-derived EVs applied to the
75 AIA model of inflammatory arthritis. We investigate amelioration of symptoms through
76 reduced swelling and histopathological improvement, and EVs influence on T cell polarisation
77 in vitro and in vivo. We hypothesise that EVs represent a potential therapeutic approach for
78 the treatment of inflammatory arthritis that may encounter less obstacles than cell therapy
79 to widespread application in the clinic.

80

81 **Results**

82 *EVs isolated through differential ultracentrifugation characterise as EVs meeting ISEV criteria*

83 All EVs isolated in this study were enriched using 100,000 x g ultracentrifugation with EV
84 pellets resuspended based on counts of source cells taken at the point of collection, with
85 resuspension at vesicles from 1.0 x 10^6 MSCs per 30µl.

86 A combination of quantitative and qualitative analyses was performed to confirm isolation of
87 EVs. EV preparations from MSCs cultured under normoxic conditions were assessed by flow
88 cytometry analysis using the MACSPlex exosome kit (Miltenyi Biotec) to identify 37 exosomal
89 surface epitopes, including characteristic exosome markers CD9, CD63 and CD81. EV
90 isolations showed elevated enrichment in mean expression values for CD9 (81.25±5.03%),
91 CD63 (94.59±2.23%) and CD81 (79.41±9.07%) (n=11) (representative example Figure S1A)
92 confirming the identity as EVs. Western blot analysis of MSC lysate and EVs (EV-NormO2) for
93 detection of Alix, a protein involved in MVB biogenesis, and cytochrome C, an ubiquitous
94 mitochondrial protein acting as negative control, showed that isolated MSC-EVs are highly
95 enriched in Alix, which is expressed by their cells of origin, but do not contain cytochrome C
96 as expected (Figure S1B). TEM imaging demonstrated the presence of spherical vesicles in
97 isolated preparations in accordance with ISEV criteria for single EVs characterisation (Figure
98 S1C). Finally, EVs were characterised for their size distribution and concentration using the
99 Nanopore technology (Izon Science). EVs preparations showed a distribution of EV sizes with
100 most prevalent diameter of ~ 200 nm with maximal diameter ~500 nm (Figure S1D-E).
101 Together, these results demonstrate that our differential ultracentrifugation methodology
102 successfully isolates EVs meeting ISEV criteria. We observed that pro-inflammatory priming
103 of MSCs using the methodology adopted here was possible for a period of 48 hours for
104 collection of CM-MSC, but extended cell culture in the presence of pro-inflammatory cocktail
105 to 72 or 96 hours resulted in consistent reductions in cell numbers below the originally seeded
106 cell numbers, suggestive of induced crisis in the cultured cells (data not shown).

107

108 *Priming of MSCs does not affect total protein content in EV cargo*

109 We set out to determine whether the total protein content in the cargo of EVs was impacted
110 by cell priming. A 4 parameter polynomial nonlinear regression of log-transformed BCA assay
111 data revealed no significant increase in total protein between conditions EV-2%O2
112 preparations (81.29±34.82 pg/1.0 x 10^6 cells; n=8) and EV-Pro-Inflam (69.09±37.38 pg/1.0 x
113 10^6 cells; n=9) compared to EV-NormO2 (40.43±14.73 pg/1.0 x 10^6 cells; n=11) ($p>0.05$, data
114 not shown).

115

116 *Application of MSC-derived EVs ameliorates histopathology and joint swelling in AIA*

117 To assess the therapeutic potential of MSC-derived EVs we introduced each of our primed
118 MSCs EVs treatments into a murine model of inflammatory arthritis and measured effects of
119 treatments on histopathological outcomes. AIA is an acute model of inflammatory arthritis
120 that typically exhibits peak joint swelling at 24 hours post induction with clinical symptoms
121 and histopathological signs that resemble rheumatoid arthritis. We have previously
122 demonstrated the efficacy of CM-MSC in ameliorating swelling in AIA[3]. In this study, we
123 compared three EV treatments to PBS only vehicle controls, measuring the reduction of joint
124 diameter from peak swelling (day 1). Local administration of EVs into joints significantly
125 reduced joint diameter post-arthritis induction, a quantitative measure proportional to joint
126 swelling. Specifically, EV-NormO2 (day 2 = 4.4±0.6mm, day 3 = 8.0±0.6mm, $p<0.01$), EV-2%O2
127 (day 2 = 7.7±0.8mm, day 3 = 11.0±0.9mm, $p<0.001$) and EV-Pro-Inflam (day 2 = 6.7±1.0mm,
128 day 3 = 11.3±0.9mm, $p<0.001$) all very significantly reduce joint swelling in comparison to PBS
129 vehicle control treatments (day 2 = 0.2±0.8mm, day 3 = 2.8±1.0mm) (Figure 1A). Reductions
130 in joint diameter from peak swelling were proportional for all treatment conditions.

131 Histopathological symptoms include immune cell infiltration into the synovium; hyperplasia
132 of the synovial membrane; and extravasation of leukocytes into the synovial joint cavity. We
133 have previously shown that the intra-articular injection of MSC conditioned medium in mice
134 with AIA ameliorates damage as observed through histopathological analysis[3]. Whilst EV-
135 2%O2 overall showed a tendency to reduce total arthritis index (AI) scores (4.92±0.84)
136 compared to controls, this was not statistically significant. For EV-NormO2, this reduced AI
137 score reflected decreases from control scores in hyperplasia of the synovial membrane
138 (1.35±0.22 vs 2.30±0.17) and joint exudate (0.50±0.21 vs 1.68±0.30), whilst EV-Pro-Inflam
139 demonstrated reduced synovial infiltrate (2.0±0.39 vs 3.49±0.24) (Figure 1B). Overall AI
140 showed significant reductions in mice treated with EV-NormO2 (4.20±0.79) and EV-Pro-Inflam
141 (4.08±1.04) compared to EV-depleted medium control (7.46±0.59) (Figure 1C). Taken
142 together, these results demonstrate EV-NormO2 treatment produced a broad reduction in
143 swelling and improvement in histological outcomes, whilst primed MSCs were effective in
144 reducing swelling, but evidence suggested this was not exclusively through reductions in
145 synovial infiltrate or reduced synovial damage.

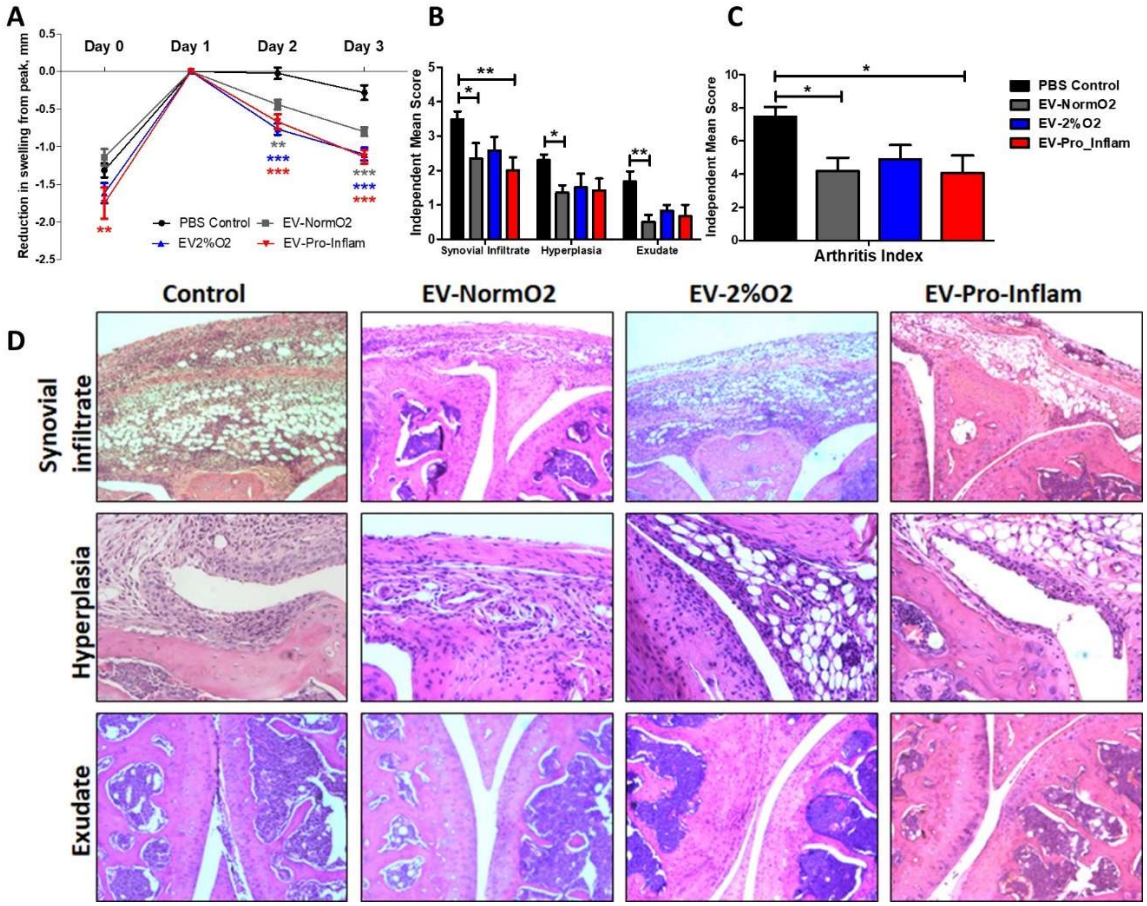

Figure 1 – MSC-derived EVs treatment of mice with AIA. (A) Alleviation of joint swelling as a measure of therapeutic efficacy following EV treatments shows a significant effect of EVs compared to vehicle controls at day 2 and day 3 after arthritis induction; normalised to 0 at peak swelling (day 1) (2 Way ANOVA with Repeated Measures and Bonferroni multiple comparisons test post hoc) (B) Examination of histological signs of arthritis pathogenesis following EV treatment shows significant therapeutic effects of EVs sourced from MSCs cultured under normoxia and MSCs cultured in the presence of pro-inflammatory cytokines 3 days post-induction. (C) Combined score arthritis index shows significant reductions in arthritis index 3 days after induction when treated with EVs (1 way ANOVA with Repeated Measures and Bonferroni Multiple Comparisons test post hoc); (D) Representative images for synovial infiltrate, hyperplasia of the synovial lining and synovial exudate into joint cavity for vehicle control and EVs treatments (Control n=21, EV-NormO2 n=8, EV-2%O2 n=6, EV-Pro-Inflam n=6. *p<0.05; **p<0.01; ***p<0.001)

EV-Pro-Inflam treatments showed reductions in synovial infiltrate sufficient to affect a significantly improved overall arthritis index, however this treatment methodology was not as effective at reducing synovial exudate or hyperplasia of the synovial membrane (Figure 1D). The reduction in synovial infiltrate may therefore contribute towards reduced swelling

164 however the results seen in EV-2%O2 suggests this is not a single factor underpinning the
165 mechanism of action.

166

167 *EV treatments do not affect expression of pro- (TNF-α) and anti-inflammatory (IL-10) cytokines*
168 *detectable in serum of AIA mice*

169 The pro-inflammatory cytokine TNF-α is a key driver of disease pathogenesis in RA and a
170 therapeutic target in biological treatments[25,26]. Conversely, IL-10 is a master regulator of anti-
171 inflammatory immune responses[6]. To investigate the effects on circulating cytokines, TNF-α
172 and IL-10 were measured at day 3 in the serum of mice following EV treatments. The
173 circulating concentration of TNF-α in serum of treated mice did not vary significantly between
174 controls (7.02±0.47pg/mL, n=15) and EV treated conditions or between treatments EV-
175 NormO2 (7.38±1.04pg/mL), EV-2%O2 (6.93±0.65pg/mL) or EV-Pro-Inflam (5.73±0.47pg/mL)
176 ($p>0.05$, n=5 per treatment). ELISA on mouse serum could not detect IL-10 in treatment or
177 control conditions (data not shown). Owing to the small volume of synovial fluid in the murine
178 articular cavity, it was not possible to isolate sufficient synovial fluid to accurately detect
179 cytokine expression within the localised joint cavity. The consistent concentrations of
180 circulating TNF-α in serum of mice undergoing treatment and in untreated control mice
181 suggests that immunomodulation of TNF-α regulated cytokine/chemokine induction is not a
182 primary mechanism underpinning efficacy of EVs treatments in reducing swelling and/or
183 histological improvement. This is in contrast to results previously observed in MSC
184 treatments[2].

185

186 *EVs with hypoxic priming or unprimed decrease Th17 polarization but only MSCs suppress*
187 *proliferation when co-cultured with activated CD4+ T cells in vitro*

188 Prior to introduction in vivo, we investigated the in vitro effect of MSC-derived EVs on T cell
189 polarisation and proliferation to establish an alternative mechanistic rationale for efficacies
190 observed in swelling and histological scores for EVs treatments. MSCs have been shown to
191 deactivate T cells in co-culture (2,3). MSCs and EVs produced following conditions EV-
192 NormO2, EV-2%O2 and EV-Pro-Inflam were therefore co-cultured for 5 days with activated T
193 cells isolated from healthy mice and polarisation and proliferation of activated cells assessed
194 as a measure of immune response and T cell deactivation.

195 T cell polarisation was assessed by flow cytometry analysis of surface CD4 and intracellular
196 markers characteristic of Th1 (IFN-γ), Th2 (IL-4) and Th17 (IL-17a). The ability of EV treatments
197 to affect deactivation of T cells, and therefore influence T cell proliferation and extent of
198 immune response, was examined to determine experimental conditions for assessment of EV
199 treatment interactions with T cells in vivo.

200 Replicating previous studies[2,3], MSC/CD4+ T cell co-cultures prompted significantly increased
201 numbers of CD4+ T cells compared to activated T cells cultured alone. MSCs also elicited
202 increased CD4+ T cells in comparison to all EV treatment conditions ($n=3$, $p<0.05$) (Figure 2A).

203 Further analysis of IL17a expressing cells within the CD4+ population demonstrated that MSC
204 co-cultures increased cell proportions in comparison to PBS controls and all EV conditions,
205 whereas all EV treatments showed a decrease in Th17 cell polarisation ($p>0.05$, $n=3$) (Figure
206 2B). Whilst no differences were seen for IFN-γ expressing cells (Th1) (Figure 2C), IL-4
207 expressing cells (Th2) were elevated in MSC co-cultures (6.00±0.24%) compared to EV-Pro-
208 Inflam (2.74±0.52%) ($p<0.01$) but not in comparison PBS control (4.79±0.99%); EV-NormO2

209 (2.86±0.30%) or EV-2%O2 (3.22±0.03%) ($p>0.05$, $n=3$) (Figure 2D). Statistical analysis was
210 performed using log transformed data.

211 Additionally, the expression of IL17a per cell, represented by mean fluorescence intensity
212 (MFI) of signal, was significantly reduced in EV-NormO2 (3311.74±33.71) and EV-2%O2/CD4+
213 T cell co-cultures (3367.19±39.92) compared to CD4+ T cells cultured alone (3728.69±50.28)
214 ($p<0.01$, $p<0.05$, $n=3$). The impact of this change would need to be assessed in vivo as this had
215 not translated to reduced Th17 numbers in vitro.

216 These results demonstrate that *in vitro* MSC-derived EVs do not prompt increases in CD4+ T
217 cell numbers or Th17 effector cell polarisation as seen with MSC treatments. Interpretation
218 of this data is limited by the lack of Treg data preventing the examination of the Treg:Th17
219 ratio which is offset in RA.

220

221 We have previously shown the ability of MSCs to suppress T cell proliferation in co-culture,
222 with MSCs being more effective than CM-MSC[2,3]. MSC/CD4+ T cell co-culture reduced the
223 proportion of proliferating T cells, measured via a proliferative index[27] and the number of
224 proliferative cycles[28] undergone by T cells in co-culture (5.31±0.38, 4.63±0.17 respectively) in
225 comparison to T cells cultured alone (6.16±0.10, 5.44±0.25) ($n=8$, $p<0.05$). In contrast, CD4+
226 T cells from healthy (not AIA induced) mice showed no significant inhibition of proliferative
227 cycles when cultured with EV-NormO2 (5.85±0.08, 5.01±0.17), EV-2%O2 (6.01±0.18,
228 4.97±0.14) or EV-Pro-Inflam (6.28±0.12, 4.95±0.09) ($n=8$, $p>0.05$) (Figure 2E).

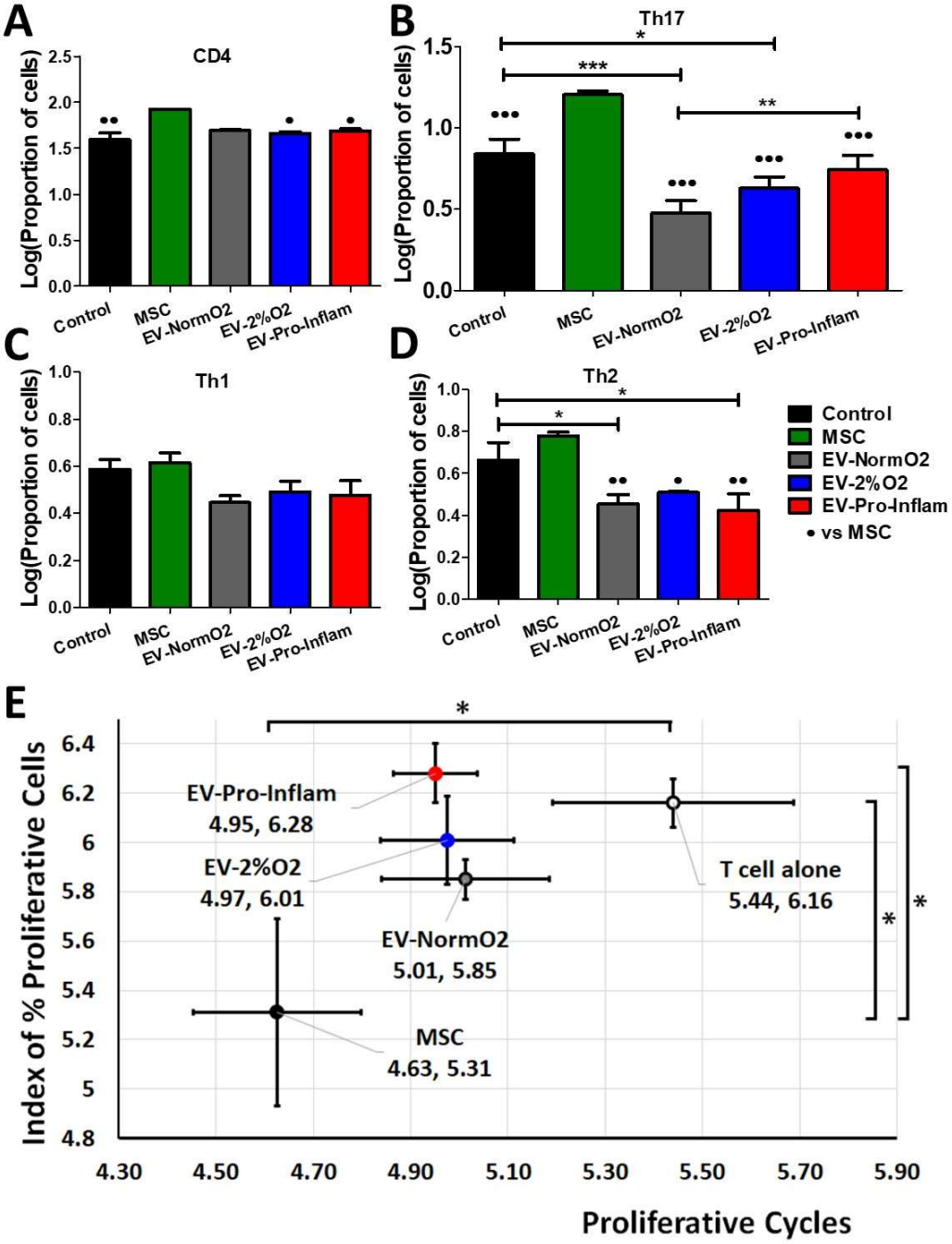

Figure 2 – Outcomes of EV treatments co-cultured with T cells isolated from healthy murine spleens **(A)** Increased CD4+ T cells in MSC co-cultures compared to EV-2%O2; EV-Pro-Inflam; and T cells alone control **(B)** Increased pro-inflammatory Th17 cells (IL17a+) in MSC co-cultures over to EV-NormO2; EV-2%O2; EV-Pro-Inflam; and T cells alone control with EV-NormO2 significantly reduced on PBS control and EV-Pro-Inflamm also **(C)** EV or MSC treatments did not alter Th1 polarisation **(D)** EV treatments all reduced Th2 polarisation in comparison to MSC treatment, with EV-NormO2 and EV-Pro-Inflam also reduced in comparison to PBS controls (Index of proliferation only) (n=3; *p<0.05; **p<0.01; ***p<0.001; 1-Way ANOVA with Bonferroni post-hoc of log transformed data. **(E)** MSC co-cultures significantly inhibited T cell proliferation compared with T cells cultured alone (both measures) and EV-Pro-Inflam co-culture (Index of proliferation only) (n=3; *p<0.05; **p<0.01; ***p<0.001; 1-Way ANOVA with Bonferroni post-hoc of log transformed data.

241 EV treatments showed greater impact on proliferative cycles than on the proliferative index,
242 though treatments did not significantly vary from either MSC co-cultures or T cells cultured
243 alone, with the exception of pro-inflammatory primed EVs which allowed a higher
244 proliferative index in comparison to MSC co-culture ($n=8$, $p<0.05$) (Figure 2E). Previous studies
245 have shown similar results through the application of whole secretome[3]. The results found
246 here suggest that direct deactivation of T cells and immunomodulated T helper polarisation
247 does not provide a primary mechanism for therapeutic action of EVs in vivo. Whilst MSCs do
248 display direct immunomodulation of T cells, it may be that MSC-secreted EVs require an
249 intermediate such as DCs to affect a similar influence on T cell responses.

250

251 *MSC-derived EVs reduce Th17 polarisation and restore the Th17:Treg balance ex vivo*

252 Following on from our in vitro study of T cell deactivation using CD4+ T cells of healthy mice,
253 we hypothesised that direct T cell interactions were not likely to be the mechanism through
254 which therapeutic effects are observed following EVs infusion. EV-Pro-Inflam treatments did
255 not influence T cell polarisation however hypoxic priming of MSCs generated EVs capable of
256 influencing Th2 polarisation and Th17 expression (observed through increased mean
257 fluorescence intensity, i.e. per cell expression). At this stage, data suggested MSC priming
258 (either 2%O2 or pro-inflammatory cocktail) conveys no beneficial advantage over
259 normoxically produced MSC-EVs in modulating T cell responses or in reducing swelling and
260 affecting improved histological outcomes. Our previous study demonstrated the ability of
261 whole secretome conditioned medium from normoxically grown MSCs to influence T cell
262 polarisation, restoring Treg:Th17 homeostasis, and to affect reductions in swelling and tissue
263 damage in vivo, similarly not via T cell deactivation when investigated in vitro[3]. We again

264 hypothesis the need for a mediating cell to affect T cell deactivation. To investigate the
265 fraction of the secretome responsible for in vivo immunomodulatory outcomes observed with
266 CM-MSC, and to reinforce the principles of 3R's, we determined to apply the AIA model to
267 examine T cell interactions in only EV-NormO2 vesicles comparative to EV depleted
268 secretome. Here we aim to elucidate whether EVs or the non-vesicular secretome affects T
269 helper cells deactivation. Spleens and lymph nodes (inguinal and popliteal) of EV-NormO2 and
270 EV-depleted CM-MSC treated AIA mice and PBS controls were dissociated, and CD4+ T cells
271 isolated. These cells represent *in vivo* primed T cells within the inflammatory arthritis
272 environment prior to EVs treatment, isolation and subsequent *in vitro* activation.

273 EV-NormO2 did not increase the proportion of CD4+ T cells in spleen (13.28±0.51%) or lymph
274 nodes (15.04±1.04%) over PBS controls in spleen (14.21±1.07%) or lymph nodes
275 (15.52±1.15%) ($p>0.05$, $n=4$). However, EV-depleted CM-MSC treatment resulted in a small
276 but statistically significant increase in the proportion of CD4+ T cells in spleens (16.94±0.81%)
277 ($p<0.05$, $n=4$) compared to EV-NormO2 treatment, but not in lymph nodes (18.83±1.13%)
278 ($p>0.05$, $n=4$) (Figure S2A, S2B shown with log transformed data).

279 Examination of *in vivo* primed CD4+ T cells activated and cultured *in vitro* for 4 hours in the
280 presence of a membrane transport blocker facilitated evaluation of T cell polarisation. These
281 results demonstrated MSC polarisation of T cells favoured Th17 outcomes as shown
282 previously[2,3]. RA (and other autoimmune disease) sufferers experience an imbalanced
283 Th17:Treg ratio leading to inappropriate immune responses and tissue damage[29-32] so for the
284 in vivo analysis we additionally examined regulatory T cells (Tregs, CD25+FOXP3+) polarisation
285 to allow calculation of ratios of Th17:Treg and Th1:Th2 to highlight differential changes in
286 polarisation of subsets of helper T cell that could affect the overall homeostatic balance.

287 When compared to PBS control (3.23±0.81%), spleen T cell polarisation towards Th17 effector
288 cells following both EV-NormO2 (0.83± 0.10%) and EV-depleted CM-MSC (0.90±0.19%)
289 treatments showed significant decreases in the proportion of pro-inflammatory Th17 cells
290 induced in AIA mice ($p<0.05$, n=4), with no significant change in FOXP3 (Treg) proportions
291 (Figure 3A). This translated to a trend for improved Treg:Th17 ratios in spleens of EV-NormO2
292 (12.06±2.12:1) and EV-depleted CM-MSC (12.70±2.95:1) treated mice compared to PBS
293 controls (5.03±1.40:1) ($p=0.12$, $p=0.09$ respectively, n=4) (Figure 3B). This result indicates that
294 EVs can prompt an advantageous shift in the Treg:Th17 balance towards a healthy state,
295 demonstrating a similar efficacy of applying EVs alone to that previously seen when applying
296 CM-MSC[3]. A similar trend was seen in T cells from lymph nodes with a significant reduction in
297 Th17 polarisation in EV (0.90±0.09%) and EV-depleted CM-MSC (0.93±0.25%) compared with
298 PBS controls (4.26±1.12%, $p<0.05$, n=4) (Figure 3C) leading to improved Treg:Th17 ratio
299 (Figure 3D). Taken together, these data show that EV treatments and EV-depleted medium
300 were both capable of affecting alleviation of symptoms of inflammatory arthritis through
301 reduced Th17 polarisation and shift in the Treg:Th17 balance. We also observed an increase
302 in pro-inflammatory Th1 cells in spleens of EV-NormO2 treated mice (6.38±0.40%) compared
303 to PBS controls (4.00±0.35%, $p<0.05$, n=4) (Figure S2C).

304 The outcomes of treatment using EVs *in vivo* demonstrate a reduction in polarisation towards
305 IL17a secreting T helper cells for both spleen and lymph nodes of AIA treated mice that is not
306 seen *in vitro* using EV-treated activated T cells from healthy mice that have not experienced
307 AIA induction. We therefore hypothesise that the therapeutic effect seen in vitro may require
308 the presence of a mediator and we propose the candidate for this would be DCs. Regulatory
309 T cells influence DCs through EVs mediated intercellular communication to provide
310 immunomodulation, including regulation of tolerance in autoimmune conditions[24].

311 Potentially the variation observed through *in vivo* treatments compared with *in vitro*

312 responses reflect the absence of mediating cell types such as DCs.

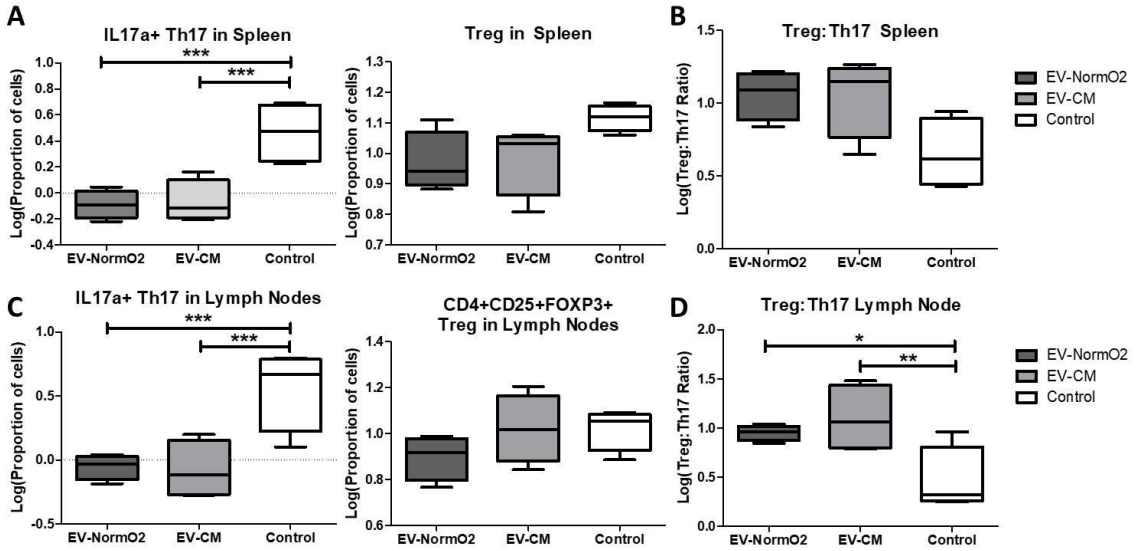

313

314 **Figure 3 – Outcomes of intracellular staining for T cell polarisation analysis. Intracellular staining**
315 **for FACS analysis of IFN-γ, IL4 and IL17a in CD4+ T cells from EV-NormO2, EV-depleted CM-MSC or**
316 **PBS control. Significant reductions in (A/C) IL17a expression suggestive of reduced Th17**
317 **polarisation in Spleen and Lymph Node with no change in regulatory T cell polarisation resulted in**
318 **(B/D) trend for restoration of the Treg:Th17 balance in EV-NormO2 treated mice which was found**
319 **significant in lymph node cells only (n=4, *p<0.05; **p<0.01; ***p<0.001)(1 Way ANOVA with**
320 **Bonferroni Multiple Comparisons Test post hoc using log transformed data.**

321

322 **Discussion**

323 This study builds on the growing knowledge for the therapeutic efficacy of EVs as a treatment

324 for inflammatory autoimmune disorders. We aim to inform researchers and clinicians on the

325 efficacy of priming strategies to prepare EVs as an enhanced therapy. In our study, EV

326 treatments prompted amelioration of clinical symptoms of AIA with reduction of joint

327 swelling both with and without priming. Examination of joint sections showed improved

328 histological features following standard and pro-inflammatory primed MSC-derived EV

329 treatments compared to controls but not when using hypoxically derived EVs.

330 Mechanistically, EVs acted remarkably different from their cells of origin (MSCs) when co-
331 cultured with CD4+ T cells from healthy murine spleens. Standard and hypoxically-derived EVs
332 reduced Th17 polarization without affecting T cell proliferation, while MSCs increased Th17
333 polarization, and lessened T cell proliferation. Our previous study indicated that MSCs do
334 indeed increase Th17 polarisation but this is offset by increases in Treg cells to restore a more
335 homeostatic balance between the two. Here we examined the Treg:Th17 ratio following AIA
336 initiation and treatment with EV-NormO2. With lack of significant improvements in hypoxic
337 priming outcomes, we opted to test only EV-NormO2 and EV-depleted CM to compare MSC-
338 CM fractions for influence on T cell polarisation following treatment application in the pro-
339 inflammatory environment. *Ex vivo*, CD4+ T cells isolated from spleens of arthritic mice
340 treated with standard EV-NormO2 again showed significantly reduced Th17 polarization that
341 rebalanced the Treg:Th17 ratio. Together, this suggests the reduction in Th17 cells led to
342 restoration of the Treg:Th17 ratio, which is typically unbalanced in inflammatory arthritis, and
343 reduced immune cell recruitment.

344 To further dissect the therapeutic mechanism of action of MSC-derived EVs, circulating levels
345 of TNF-α, which is a key driver of pathogenesis in RA and therapeutic target in biological
346 treatments, and IL-10, which is a master regulator of anti-inflammatory immune responses,
347 were measured in mice with AIA at day 3. While IL-10 was not detected in our assay, similarly
348 low levels of TNF-α were detected in serum of untreated and EV-treated mice. However,
349 whilst this suggests that TNF-α blockade and IL-10 modulation are not the mechanisms by
350 which MSC-derived EVs improve AIA, it is noted that circulating serum levels of TNF-α rise
351 rapidly in 24 hours post-induction then fall rapidly in the AIA model, so detectable serum TNF-
352 α may not be significantly different in AIA and control mice at 3 days post-induction[33,34]. This

353 mechanism may be more suited to assessment following prophylactic treatment using EVs
354 administered at the point of induction rather than after onset of symptoms.

355 Our previous study demonstrated reductions in Th17 cells following CM-MSC treatment
356 compared to control and MSC treatments. Whilst EVs have been shown to increase Il-10 in
357 macrophages[35], this study indicates that the presence of MSCs, and not just their secretome,
358 may be driving increased IL-10 expression influencing T cell polarisation in vivo, and were
359 responsible for the reduction in Th1 and increase in Th2 cells seen in our previous study[3]. EVs
360 are capable of significantly reducing Th17 cell numbers however and this represents a
361 significant finding in the search for immunomodulatory therapeutics for treating autoimmune
362 disorders where an imbalance in T cell polarisation (Th1:Th2 or Treg:Th17) is integral in
363 disease pathology. Moreover, EV treatment in this study resulted in an improved (2.40-fold
364 over controls) Treg:Th17 ratio compared to our previous results using whole CM-MSC
365 treatment (2.13-fold over control) or MSC treatment (1.47-fold over control)[3].

366 The proportions of Treg and Th17 cells in RA sufferers has been directly linked to the severity
367 of disease, and restoring the Treg:Th17 balance has the potential to promote homeostasis
368 and positive clinical outcomes. Here, we demonstrate that untreated (PBS control) spleens of
369 mice with AIA display a Treg:Th17 ratio of 5:1 and that this is improved to 12:1 upon EV-
370 NormO2 and control EV-depleted CM-MSC treatments. This result reinforces the use of CM-
371 MSC or vesicular components as a therapeutic option for RA treatment.

372 We observed effects on T cell polarisation that were consistent between in vitro and ex vivo
373 outcomes, with the exception of reduced Th2 cells in vitro unmatched ex vivo.

374 It has been suggested that the immunomodulatory properties of EVs are contingent on pro-
375 inflammatory priming[19,36]. However, the present work demonstrates that whilst priming

376 strategies may enhance some therapeutic outcomes, the mechanisms are unclear and the
377 overall immunomodulatory property may be inherent to MSC-EVs regardless of priming
378 methodology. EV-Pro-Inflam were the least effective treatment methodology for T cell
379 deactivation however did reduce swelling and immune cell recruitment to the synovium. In
380 contrast, hypoxically primed MSCs produced EVs that reduced swelling but failed to have any
381 impact upon the histological outcomes measured in AIA joints.

382 Our results suggest that the *in vivo* response to pro-inflammatory primed EV treatment in the
383 AIA model of inflammatory arthritis is not primarily through inhibition of T cell activation, but
384 through suppression of CD4+ Th17 effector polarisation combined with reduction in synovial
385 infiltration through reduced recruitment of immune cells to the affected joint. Although this
386 effect is more pronounced following pro-inflammatory priming of MSCs in comparison to
387 standard EV production, the reduction in exudate and hyperplasia seen with EV-NormO2
388 treatments is likely to convey a greater therapeutic response. Pannus tissue is thought to
389 develop from cells of the synovial membrane and cells infiltrating the joint cavity in response
390 to pro-inflammatory signalling[37,38]. The reduction of synovial infiltrate, hyperplasia and
391 synovial exudate observed in EV-NormO2 treatments in vivo may therefore translate to
392 reduced pannus formation. These benefits, in combination with Th17 modulation and
393 improved Th17:Treg balance would convey advantageous outcomes in comparison to either
394 priming methodology.

395 We hypothesise that whilst the overall effectiveness of these treatment methodologies is
396 similar in potency, the outcomes differ due to variations in underlying mechanisms of action.
397 Our results demonstrate hypoxic preconditioning reduces swelling in vivo and affects Th17
398 polarisation of T cells in vitro, however insufficient evidence was found to propose a clear

399 mechanism for therapeutic capacity. MSCs under hypoxic culture have been shown to
400 promote anti-inflammatory M2 macrophage polarization[39], reduce reactive oxygen species
401 (ROS) and upregulate TGF-β, IL-8, IL-10 and PGE2, which are also implicated in macrophage
402 polarisation and MSC immunomodulatory capacity[39-41]. Consequently, we hypothesise that
403 effects seen in vivo following hypoxic preconditioning may be related to reduction in
404 macrophage mediated immune responses and more appropriate for tissue regenerative
405 applications. Furthermore, hypoxic culture of MSCs has been shown to promote
406 vascularisation[42,43] which, whilst beneficial for tissue repair, may actually contribute to
407 pannus formation in the RA joint[38]. Given these considerations, the evidence here suggests
408 that normal culture conditions are sufficient to elicit an optimal response in MSCs for EVs
409 production ahead of therapeutic application into the inflammatory environment.

410 Previously, we determined that joint swelling in induced arthritis as a clinical indication of
411 joint inflammation is reduced in the presence of administered MSCs and these cells migrate
412 into the inflamed synovium[2]. Joint swelling is common with different types of arthritis and is
413 caused by oedema due to the endothelial cells of blood vessels becoming leaky in the
414 inflamed synovium. We hypothesised that soluble factors produced by MSCs are responsible
415 for permeability changes in the synovial endothelial cells as these cells did not co-localise,
416 although further studies are required in this regard. The therapeutic potential of MSC-derived
417 EVs has been documented in animal model of radiation-induced lung injury where EVs
418 attenuated radiation-induced lung vascular damage, inflammation, and fibrosis via miRNA-
419 214-3p[44] and in a rodent model of haemorrhagic shock-induced lung injury model where EVs
420 attenuated pulmonary vascular permeability and lung injury[45].

421 Given the observed outcomes, we hypothesise that the similarities in immunomodulation
422 between EV-2%O2 and EV-Pro-Inflam treatment may lie in their influence on STAT3
423 activation. Increased HIF-1α activates STAT3[46]. STAT3 induces RORγt expression and is
424 activated by TNF-α, IL-6, IL-21 and IL-23, which are key cytokines in promoting Th17
425 differentiation, and RORγt is a master regulator of Th17 differentiation[47,48]. Moreover, STAT3
426 activation has been shown to be necessary for the development of Th17 cells and Th17
427 related autoimmunity, such as seen in RA[48] so EVs inhibiting STAT3 activation could lead to
428 the drop in Th17 polarisation observed. EVs from other mesenchymal cell types are implicated
429 in influencing STAT3 signalling to induce mesenchymal transition[49] and EVs from
430 macrophages are able to trigger nuclear translocation of STAT-3[35], demonstrating STAT3
431 activation as a target of EVs influence. STAT3 has been suggested as a therapeutic target in
432 the treatment of autoimmune inflammatory disorders such as RA[50] and inhibition of STAT3
433 by EVs would have direct therapeutic potential. Further work can elucidate this mechanism of
434 action.

435 In this study, our primary aim was to evaluate the efficacy of EV treatments *in vivo* during AIA.
436 We show that MSC priming leads to the release of EVs that if administered to mice with acute
437 inflammatory arthritis significantly ameliorate disease pathogenesis, mainly by inhibiting
438 Th17 polarization. Future studies will define the composition and sub-vesicular localisation of
439 proteins in EV cargos.

440

441 ***Conclusions***

442 This study provides new evidence that supports the use of EVs in clinical therapies for RA and
443 similar autoimmune disorders. The possibility to manipulate the protein and nucleic acid

444 cargo of EVs through control of parental MSC cultures offers a novel opportunity for targeted
445 therapies that can be tailored to individual pathological features of RA, advancing
446 personalised medicine. Further work on the control of EV cargo will elucidate the molecular
447 mechanism of action underlying varied responses between priming strategies and assist in
448 the efficacy of cell-based therapies in the clinic. This study aims to support the growing body
449 of evidence for the introduction of EVs into the therapeutic milieu.

450

451 **Methods**

452 *Cells and EVs*

453 Primary human MSCs were isolated from commercially available bone marrow aspirate
454 (Lonza, USA) using an adherence technique[40] and each donor material cultured in both
455 normoxic (21%O_2) or hypoxic (2%O_2) conditions from isolation of MSCs in Dulbecco's
456 Modified Eagles Medium (DMEM) with 10% foetal bovine serum (FBS) and 1% penicillin-
457 streptomycin (n=3). Hypoxic cell culture was achieved using 2% O_2 in hypoxic workstation
458 (Invivo$_2$ Physiological Cell Culture Workstation, Baker Ruskinn) to ensure cells were not
459 exposed to environmental oxygen levels at any stage of isolation or culture. Cells (P3-P5) were
460 characterised as MSC through immunophenotyping of surface markers with flow cytometry
461 and tri-lineage differentiation[2]. EVs were therefore isolated over a 48 hour culture period
462 from MSCs in normoxic 21% oxygen culture (EV-NormO2, n=11); MSCs in hypoxic 2% oxygen
463 culture (EV-2%O2, n=4) and from MSCs previously cultured for 48 hours with pro-
464 inflammatory cytokine cocktail comprising interferon-gamma (IFN-γ, 10ng/ml), tumour
465 necrosis factor-alpha (TNFα, 10ng/ml) and interleukin 1 beta (IL-1β, 5ng/ml) prior to transfer
466 to serum-free medium for 48 hours for EV collection (EV-Pro-Inflam, n=4).

467

468 *Differential ultracentrifugation for isolation of EVs*

469 MSCs from the same batch used for cell treatment (P3-P5) were cultured to 80-90%
470 confluence in T75 flasks, washed with PBS three times and then serum-free DMEM. Flasks
471 were incubated for 48 hours with 12ml serum-free DMEM at 37°C, 5% CO_2. After 48 hours,
472 conditioned medium (CM-MSC) was removed and a cell count performed to determine the
473 number of cells used to produce EVs. EVs were isolated from CM-MSC by differential
474 ultracentrifugation. In brief, CM-MSC was centrifuged for 10 minutes at 300 *x g* to remove
475 cell debris then again for 10 minutes at 2000 *x g* to remove apoptotic bodies and residual
476 dead cells. Supernatant was again taken and centrifuged at 10,000 *x g* for 45 minutes in an
477 ultracentrifuge (Beckman Coulter) to remove larger/denser EVs. Supernatant was again
478 retrieved and passed through a 0.22µM syringe filter. Filtered supernatant was then
479 centrifuged using 70.1Ti rotor (Beckman Coulter) in a Beckman L8-55M ultracentrifuge at
480 100,000 *x g* for 90 minutes to isolate a pellet comprising small EVs. EVs depleted medium
481 supernatant was removed and stored at -20°C (EVs-depleted CM-MSC), whilst the visible EVs
482 pellet was resuspended in 5ml of PBS to wash EVs and then spun again at 100,000 *x g* for 60
483 minutes, the supernatant discarded and the residual EV pellet resuspended in PBS at 30µL per
484 1.0 x 10^6 cells used in EV generation and stored at 4°C to be used within 24 hours or at -20°C
485 for later use.

486

487 *Characterisation of EVs*

488 Successful isolation of EVs was confirmed through multiple methods in accordance with ISEV
489 guidelines[51]. Samples of vesicle preparations underwent bicinchoninic acid assay (BCA Assay,

490 Pierce Biotechnology) for total protein concentration in EV preparations following
491 manufacturer's instructions with EV disruption in a sonicating water bath (30 seconds
492 sonication at 1 minute intervals for 3 cycles) to release intracellular protein and assess cargo
493 proteins as well as surface proteins. Data passed a Kolmogorov-Smirnov test for normality
494 and was analysed with a repeated measures 1 way ANOVA with Tukey's post hoc multiple
495 comparison test.

496 Vesicles were examined using flow cytometry for expression of characteristic markers CD9,
497 CD63 and CD81 (Miltenyi MACSPlex Exosome Identification Kit, human) following
498 manufacturer's instructions for analysis. Particle by particle analysis of vesicle size was
499 assessed using Nanopore technology (Izon Science Ltd) tuned in the region ~80-300nm, to
500 confirm the size fractions being applied experimentally.

501 Images of EVs were obtained using Transmission Electron Microscopy (TEM). EVs to be
502 imaged by TEM were isolated as detailed above, however residual EV pellet after PBS wash
503 was resuspended in 30µl Milli-Q water per 3.0 x 10^6 cells. The resulting EV suspension was
504 spotted onto a glow discharged holey carbon mesh copper grids (Quantifoil, R2/1) and
505 incubated at room temperature for 4 mins 45 seconds before 5µL of 0.22µm filtered 2% (v/v)
506 uranyl acetate was added. This was left to incubate at room temperature for a further 90
507 seconds before the excess liquid was removed using blotting paper. Grids were then imaged
508 using a FEI Tecnai G2 12 Biotwin (LaB_6, accelerating voltage 100kV).

509 EV protein content was examined by Western Blotting to identify the presence of Alix and
510 absence of mitochondrial Cytochrome C (CYC1) in isolated particles, as per the minimal
511 criteria for identification of EVs[52]. Briefly, ten micrograms of EVs and cells were lysed with 2x
512 Laemlli buffer with β-mercaptoethanol and denatured by heating at 70°C for 5min. Samples

513 were electrophoresed on a 4-12% TGX stain free gel (Bio-Rad, CA, USA) at 200V for 30-40min.
514 Samples were then blotted onto a nitrocellulose membrane using the wet transfer method
515 overnight at 100V. After blotting, membranes were blocked for 2 hours in 5% semi-skimmed
516 milk in Tris-buffered saline with 0.05% Tween (TBST) followed by an incubation in primary
517 antibodies Alix (1:200), CYC1 (1:200) (Santa Cruz Biotechnology, TX, US) for 2 hours at RT.
518 After three five-minute washes, the membrane was probed with a goat anti-mouse IgG-HRP
519 conjugated secondary antibody (1:1,000 in TBST, Life Technologies Limited, Paisley, UK). HRP-
520 conjugated secondary antibody was added for 1h and the wash step repeated. SuperSignal
521 West Femto Chemiluminescent Substrate (Thermo Fisher Scientific, Waltham, MA, USA) was
522 added to the membrane and imaged with ChemiDoc™ Touch Imaging System (Bio-Rad, CA,
523 USA) using Image Lab v.6.0.1 software (Bio-Rad, CA, USA).

524

525 *Co-culture of healthy T cells with EVs*

526 Proliferation of activated T cells was assessed as a measure of T cell deactivation. Initially, for
527 positive controls $5x10^4$ MSCs were cultured in 96-well plates for 24 hours at 37°C. CD4+ T cells
528 were purified from spleens and lymph nodes (popliteal/inguinal) of healthy C57Bl/6 mice
529 using the CD4+ T Cell Isolation Kit (Miltenyi) following manufacturer's instructions. T cells
530 were seeded at a density of $5.0x10^5$/well in 250µl RPMI medium with 10% FBS and cultured
531 for 5 days with MSCs (ratio 10:1) or with EV-NormO2, EV-2%O2 or EV-Pro-Inflam (ratio
532 equivalent to secretions from 10:1 cells) (n=8). T cells alone served as control. Cells were
533 activated using anti-Biotin MACSiBead Particles (Miltenyi) (ratio 2:1). EV treatments were
534 refreshed after 2 days of culture. Polarisation was assessed as above and proliferation
535 measured through reduction in signal intensity using VPD450 Violet proliferation dye (BD

536 Biosciences)[3]. Data was analysed using a 2 way repeated measures ANOVA with Bonferroni
537 multiple comparison test post hoc.

538

539 *Antigen-induced arthritis (AIA) model of inflammatory arthritis*

540 Animal procedures were undertaken in accordance with Home Office project licence
541 PPL40/3594. AIA was induced in male C57Bl/6 mice (7-8 weeks) as previously described[2,3,53].
542 Swelling was assessed by measuring the difference in diameter between the arthritic (right)
543 and non-arthritic (left) knee joints (in mm) using a digital micrometer (Kroeplin GmbH) before
544 and at set time points after treatment. Independent experiments were performed to assess
545 swelling and histopathological effects of EV-NormO2 (n=10), EV-2%O2 (n=6) and EV-Pro-
546 Inflam (n=6) compared with PBS controls (n=21) with all EVs sourced from matching MSCs
547 and statistical analysis performed using 2 Way ANOVA for Repeated Measures with
548 Bonferroni Multiple Comparisons Test post hoc; or to for in vivo primed T cell collections using
549 EV-NormO2 compared with EV-depleted CM-MSC (matched origin) with PBS control (n=4)
550 and log transformed data analysed with 1-Way ANOVA with Bonferroni Multiple Comparisons
551 Test post hoc.

552 Peak swelling was observed at 24 hours post-induction and results at subsequent timepoints
553 are expressed in millimetres as reduction from peak swelling.

554

555 *Intra-articular injection of EVs*

556 Treatments comprised 15µl of EVs suspension corresponding to EV secretions from ~5.0 x 10^5
557 cells, or EV-depleted CM-MSC (basal medium using serum free DMEM). Treatments or PBS

558 vehicle control were injected intra-articularly 1 day post arthritis induction with 0.5ml
559 monoject (29G) insulin syringes (BD Micro-Fine, Franklyn Lakes, USA) through the patellar
560 ligament into the right knee joint. Joint diameters were measured at 1, 2 and 3 days post
561 injection. Blood, joints, spleen, inguinal and popliteal lymph nodes were collected
562 immediately post-mortem. Four independent experiments were performed to assess primed
563 EVs impact on joint swelling and histopathology (Control n=21, EV-NormO2 n=10, EV-2%O2
564 and EV-Pro-Inflam n=6). A further independent experiment was conducted to address the
565 mechanism behind conditioned medium efficacy in immunomodulation of T cell polarisation
566 in AIA by specifically identifying the contribution of EVs to secretomic effects (EV-NormO2
567 versus EV-depleted conditioned medium with PBS controls, n=4 per condition). All measures
568 were taken to reduce animal numbers wherever possible.

569

570 *Arthritis Index*

571 Animals were sacrificed for histological analysis at day 3 post arthritis induction. Joints were
572 fixed in 10% neutral buffered formal saline and decalcified in formic acid for 4 days at 4°C
573 before paraffin embedding. Sections (5µm) were stained with haematoxylin and eosin (H&E)
574 and mounted in Hydromount (National Diagnostics) as described previously[2,3]. H&E sections
575 were scored for hyperplasia of the synovial intima (0=normal to 3=severe), cellular exudate
576 (0=normal to 3=severe) and synovial infiltrate (0=normal to 5=severe) by two independent
577 observers blinded to experimental groups[54]. Scores were summated, producing a mean
578 arthritis index. Data was analysed using a 1 way repeated measures analysis of variance test
579 with Bonferroni multiple comparison test post hoc.

580

581 *Cytokine Quantification.*

582 IL-10 and TNFα in serum and CM-MSC were quantified using mouse Quantikine ELISA IL-10
583 immunoassay (R&D Systems) and TNFα ELISA high sensitivity (eBioscience) respectively,
584 following manufacturer's instructions.

585

586 *T cell polarisation*

587 Spleens and lymph nodes (popliteal/ inguinal) were collected from mice 3 days post-arthritis
588 induction and dissociated as described previously[3]. Splenocytes and pooled lymph node cells
589 were seeded separately at 1.0×10^6 cells/well in 96-well plates (Sarstedt) in RPMI-1640 with
590 10% FBS, 0.05µg/mL IL-2 and activated with cell stimulation cocktail (eBioscience) for 1 hour
591 prior to adding 10µg/ml brefeldin A (Sigma) and culturing for a further 4 hours. Unstimulated
592 T cells and cells without brefeldin A served as negative controls. Following activation, cells
593 were resuspended in 2mM EDTA in PBS and Tregs (CD4+CD25+FOXP3+) were isolated using
594 the CD4+CD25+ Regulatory T Cell Isolation Kit (Miltenyi) following manufacturer's
595 instructions; or stained for T cell subset identification. For this, cells were permeabilised using
596 permeabilisation buffer kit (eBioscience) and intracellularly stained with anti-mouse IFN-γ
597 (Th1), IL-4 (Th2) or IL17a (Th17) (eBioscience). Cells were analysed on a BD FACS Canto II flow
598 cytometer and comparisons drawn for percentage CD4+ cells and signal intensity (XGeoMean)
599 for each antibody.

600

601 *Statistical analysis*

602 Data were tested for equal variance and normality using D'Agostino & Pearson omnibus
603 normality test. Differences between groups were compared using 1-way ANOVA with
604 Bonferroni post hoc for parametric data or Kruskal-Wallis ANOVA with Dunn's post hoc test
605 for non-parametric, or 2-way ANOVA with Bonferroni correction, as stated. Repeated
606 measures tests using log transformed data was applied to Protein concentration was analysed
607 with log transformed data using a 4 parameter polynomial nonlinear regression to interpolate
608 results from a standard curve. All statistical analysis was carried out using Prism 5 (GraphPad
609 software) or IBM SPSS Statistics 24.0, with $P<0.05$ deemed statistically significant. Results are
610 expressed as mean ± standard error of the mean.

611

612 ***List of abbreviations***

613 *AIA – Antigen Induced Arthritis model*

614 *BCA – Bicinchoninic Acid Protein Assay*

615 *CM-MSC – MSCs derived conditioned medium*

616 *CTSD – Cathepsin D*

617 *CYC1 – Cytochrome C*

618 *DMEM – Dulbecco's Modified Eagle's Medium*

619 *EV-2%O2 – EVs derived from cells cultured in 2% oxygen*

620 *EV-NormO2 – EVs derived from cells cultured in normal environmental oxygen ~21%*

621 *EV-Pro-Inflam – EVs derived from MSCs cultured with pro-inflammatory cytokine stimulation*

622 *EVs – Extracellular vesicles*

623 *FBS – Foetal bovine serum*

624 *FIH – Factor inhibiting Hif-1 protein*

625 *H&E – Haematoxylin and eosin stain*

626 *HIF-1α – Hypoxia inducible factor 1 alpha*

627 *ICAM-1 – Intercellular adhesion molecule 1*

628 *IDO – Indoleamine 2,3-dioxygenase*

629 *IFN-γ – Interferon gamma*

630 *IL-10 – Interleukin 10*

631 *IL-1β – Interleukin 1 beta*

632 *ISEV – International Society of Extracellular Vesicles*

633 *LFA-1 – Leukocyte function associated antigen 1*

634 *MFI – Mean fluorescence intensity*

635 *miRNA – micro ribonucleic acid*

636 *MMPs – Matrix metalloproteins*

637 *MSCs – Mesenchymal stem/stromal cells*

638 *MVBs/MVEs – Multivesicular bodies/endosomes*

639 *NO – Nitric oxide*

640 *PBS – Phosphate buffered saline*

641 *RA – Rheumatoid Arthritis*

642 *RF – Rheumatoid factor*

643 *RISC – RNA-induced silencing complexes*

644 *RORγt – Retinoic acid receptor-related orphan receptor-γt*

645 *ROS – Reactive oxygen species*

646 *TIMPs – Tissue inhibitor of metalloproteinases*

647 *TNF-α – Tissue necrosis factor alpha*

648 *Treg – Regulatory T cell*

649 *VEGF – Vascular endothelial growth factor*

650 *VHL – von Hippel-Lindau ubiquitin ligase*

651 ***Acknowledgements***

652 The authors would like to thank the Nanoscale and Microscale Research Centre, University of
653 Nottingham, for access to TEM facilities. We would like to thank Dr. Mark Platt (Loughborough
654 University, UK) for his assistance in Nanopore technology.

655 ***Declaration of Interest Statement***

656 The authors declare that they have no competing interests

657 ***Funding***

658 This work was supported by the RJAH Orthopaedic Hospital Charity under Grant [G08028];
659 the UK EPSRC/MRC CDT in Regenerative Medicine (Keele University, Loughborough
660 University, the University of Nottingham) under Grant [EP/F500491/1]; Orthopaedic
661 Institute, Ltd under Grant [RPG 171].

662 ***Author's contributions***

663 A.K. performed experimental work, wrote the manuscript and prepared all figures. K.T.
664 provided support and technical skills for T cell investigations. P.R. gave technical expertise
665 on Nanopore technology. R.M. provided support for histological investigations, TEM
666 experiments and discussed and commented on the manuscript. R.L. performed TEM
667 experiments. M.H. performed ELISAs and provided support for *in vivo* work and histological
668 experiments. A.M.P. gave technical advice on data interpretations and presentation and
669 reviewed the manuscript. N.R.F. contributed to experimental design. O.K. conceived and
670 designed the research study, performed *in vivo* experiments, analysed data, wrote and
671 supervised the manuscript. All authors reviewed the manuscript before submission.

672 **References**

673 1 Prockop, D. J. & Oh, J. Y. Mesenchymal stem/stromal cells (MSCs): role as guardians of
674 inflammation. *Mol Ther* **20**, 14-20, doi:10.1038/mt.2011.211 (2012).
675 2 Kehoe, O., Cartwright, A., Askari, A., El Haj, A. J. & Middleton, J. Intra-articular injection of
676 mesenchymal stem cells leads to reduced inflammation and cartilage damage in murine
677 antigen-induced arthritis. *J Transl Med* **12**, 157, doi:10.1186/1479-5876-12-157 (2014).
678 3 Kay, A. G. *et al.* Mesenchymal Stem Cell-Conditioned Medium Reduces Disease Severity and
679 Immune Responses in Inflammatory Arthritis. *Sci Rep* **7**, 18019, doi:10.1038/s41598-017-
680 18144-w (2017).
681 4 Stanton, H. *et al.* ADAMTS5 is the major aggrecanase in mouse cartilage in vivo and in vitro.
682 *Nature* **434**, 648-652 (2005).
683 5 Beer, K. B. *et al.* Extracellular vesicle budding is inhibited by redundant regulators of TAT-5
684 flippase localization and phospholipid asymmetry. *Proc Natl Acad Sci U S A* **115**, E1127-
685 E1136, doi:10.1073/pnas.1714085115 (2018).
686 6 Couper, K. N., Blount, D. G. & Riley, E. M. IL-10: the master regulator of immunity to
687 infection. *J Immunol* **180**, 5771-5777, doi:10.4049/jimmunol.180.9.5771 (2008).
688 7 Kusuma, G. D. *et al.* To Protect and to Preserve: Novel Preservation Strategies for
689 Extracellular Vesicles. *Front Pharmacol* **9**, 1199, doi:10.3389/fphar.2018.01199 (2018).
690 8 Muralidharan-Chari, V., Clancy, J. W., Sedgwick, A. & D'Souza-Schorey, C. Microvesicles:
691 mediators of extracellular communication during cancer progression. *J Cell Sci* **123**, 1603-
692 1611, doi:10.1242/jcs.064386 (2010).
693 9 Raposo, G. & Stoorvogel, W. Extracellular vesicles: exosomes, microvesicles, and friends. *J*
694 *Cell Biol* **200**, 373-383, doi:10.1083/jcb.201211138 (2013).
695 10 Burbano, C. *et al.* Extracellular vesicles are associated with the systemic inflammation of
696 patients with seropositive rheumatoid arthritis. *Sci Rep* **8**, 17917, doi:10.1038/s41598-018-
697 36335-x (2018).

11 Arntz, O. J. *et al.* Rheumatoid Arthritis Patients With Circulating Extracellular Vesicles Positive for IgM Rheumatoid Factor Have Higher Disease Activity. *Front Immunol* **9**, 2388, doi:10.3389/fimmu.2018.02388 (2018).

12 Messer, L. *et al.* Microparticle-induced release of B-lymphocyte regulators by rheumatoid synoviocytes. *Arthritis Res Ther* **11**, R40, doi:10.1186/ar2648 (2009).

13 Lo Cicero, A., Majkowska, I., Nagase, H., Di Liegro, I. & Troeberg, L. Microvesicles shed by oligodendroglioma cells and rheumatoid synovial fibroblasts contain aggrecanase activity. *Matrix Biol* **31**, 229-233, doi:10.1016/j.matbio.2012.02.005 (2012).

14 Zhang, H. G. *et al.* A membrane form of TNF-alpha presented by exosomes delays T cell activation-induced cell death. *J Immunol* **176**, 7385-7393, doi:10.4049/jimmunol.176.12.7385 (2006).

15 Kim, S. H. *et al.* Exosomes derived from IL-10-treated dendritic cells can suppress inflammation and collagen-induced arthritis. *J Immunol* **174**, 6440-6448, doi:10.4049/jimmunol.174.10.6440 (2005).

16 Lee, C. *et al.* Exosomes mediate the cytoprotective action of mesenchymal stromal cells on hypoxia-induced pulmonary hypertension. *Circulation* **126**, 2601-2611, doi:10.1161/CIRCULATIONAHA.112.114173 (2012).

17 Mokarizadeh, A. *et al.* Microvesicles derived from mesenchymal stem cells: potent organelles for induction of tolerogenic signaling. *Immunol Lett* **147**, 47-54, doi:10.1016/j.imlet.2012.06.001 (2012).

18 Zhang, B. *et al.* Mesenchymal stem cells secrete immunologically active exosomes. *Stem Cells Dev* **23**, 1233-1244, doi:10.1089/scd.2013.0479 (2014).

19 Cosenza, S. *et al.* Mesenchymal stem cells-derived exosomes are more immunosuppressive than microparticles in inflammatory arthritis. *Theranostics* **8**, 1399-1410, doi:10.7150/thno.21072 (2018).

20 Alcaraz, M. J., Compan, A. & Guillen, M. I. Extracellular Vesicles from Mesenchymal Stem Cells as Novel Treatments for Musculoskeletal Diseases. *Cells* **9**, doi:10.3390/cells9010098 (2019).

21 Ma, D. *et al.* Immunomodulatory effect of human umbilical cord mesenchymal stem cells on T lymphocytes in rheumatoid arthritis. *Int Immunopharmacol* **74**, 105687, doi:10.1016/j.intimp.2019.105687 (2019).

22 Thery, C., Ostrowski, M. & Segura, E. Membrane vesicles as conveyors of immune responses. *Nat Rev Immunol* **9**, 581-593, doi:10.1038/nri2567 (2009).

23 Nolte-'t Hoen, E. N., Buschow, S. I., Anderton, S. M., Stoorvogel, W. & Wauben, M. H. Activated T cells recruit exosomes secreted by dendritic cells via LFA-1. *Blood* **113**, 1977-1981, doi:10.1182/blood-2008-08-174094 (2009).

24 Tung, S. L. *et al.* Regulatory T cell-derived extracellular vesicles modify dendritic cell function. *Sci Rep* **8**, 6065, doi:10.1038/s41598-018-24531-8 (2018).

25 Djouad, F. *et al.* Reversal of the immunosuppressive properties of mesenchymal stem cells by tumor necrosis factor alpha in collagen-induced arthritis. *Arthritis Rheum* **52**, 1595-1603, doi:10.1002/art.21012 (2005).

26 Firestein, G. S. Rheumatoid arthritis in a mouse? *Nat Clin Pract Rheumatol* **5**, 1, doi:10.1038/ncprheum0973 (2009).

27 Angulo, R. & Fulcher, D. A. Measurement of Candida-specific blastogenesis: comparison of carboxyfluorescein succinimidyl ester labelling of T cells, thymidine incorporation, and CD69 expression. *Cytometry* **34**, 143-151 (1998).

28 Que, J., Lian, Q., El Oakley, R. M., Lim, B. & Lim, S.-K. PI3 K/Akt/mTOR-mediated translational control regulates proliferation and differentiation of lineage-restricted RoSH stem cell lines. *Journal of Molecular Signaling* **2**, doi:10.1186/1750-2187-2-9 (2007).

29 Al-Zifzaf, D. S. *et al.* FoxP3+T regulatory cells in Rheumatoid arthritis and the imbalance of the Treg/TH17 cytokine axis. *The Egyptian Rheumatologist* **37**, 7-15, doi:10.1016/j.ejr.2014.06.004 (2015).
30 Arroyo-Villa, I. *et al.* Frequency of Th17 CD4+ T cells in early rheumatoid arthritis: a marker of anti-CCP seropositivity. *PLoS One* **7**, e42189, doi:10.1371/journal.pone.0042189 (2012).
31 Diller, M. L., Kudchadkar, R. R., Delman, K. A., Lawson, D. H. & Ford, M. L. Balancing Inflammation: The Link between Th17 and Regulatory T Cells. *Mediators of Inflammation* **2016**, 1-8, doi:10.1155/2016/6309219 (2016).
32 Noack, M. & Miossec, P. Th17 and regulatory T cell balance in autoimmune and inflammatory diseases. *Autoimmun Rev* **13**, 668-677, doi:10.1016/j.autrev.2013.12.004 (2014).
33 Lewthwaite, J. *et al.* Role of TNF alpha in the induction of antigen induced arthritis in the rabbit and the anti-arthritic effect of species specific TNF alpha neutralising monoclonal antibodies. *Ann Rheum Dis* **54**, 366-374, doi:10.1136/ard.54.5.366 (1995).
34 Kobayashi, H. *et al.* Antigen induced arthritis (AIA) can be transferred by bone marrow transplantation: Evidence that interleukin 6 is essential for induction of AIA. *Journal of Rheumatology* **29**, 1176-1182 (2002).
35 Bellmunt À, M., López-Puerto, L., Lorente, J. & Closa, D. Involvement of extracellular vesicles in the macrophage-tumor cell communication in head and neck squamous cell carcinoma. *PLoS One* **14**, e0224710, doi:10.1371/journal.pone.0224710 (2019).
36 Maumus, M. *et al.* Utility of a Mouse Model of Osteoarthritis to Demonstrate Cartilage Protection by IFNgamma-Primed Equine Mesenchymal Stem Cells. *Front Immunol* **7**, 392, doi:10.3389/fimmu.2016.00392 (2016).
37 Fassbender, H. G. & Simmling-Annefeld, M. The potential aggressiveness of synovial tissue in rheumatoid arthritis. *The Journal of Pathology* **139**, 399-406, doi:https://doi.org/10.1002/path.1711390314 (1983).
38 Shiozawa, S., Shiozawa, K. & Fujita, T. Morphologic observations in the early phase of the cartilage-pannus junction. Light and electron microscopic studies of active cellular pannus. *Arthritis Rheum* **26**, 472-478, doi:10.1002/art.1780260404 (1983).
39 Takizawa, N. *et al.* Bone marrow-derived mesenchymal stem cells propagate immunosuppressive/anti-inflammatory macrophages in cell-to-cell contact-independent and -dependent manners under hypoxic culture. *Exp Cell Res* **358**, 411-420, doi:10.1016/j.yexcr.2017.07.014 (2017).
40 Kay, A. G. *et al.* BMP2 repression and optimized culture conditions promote human bone marrow-derived mesenchymal stem cell isolation. *Regen Med* **10**, 109-125, doi:10.2217/rme.14.67 (2015).
41 Li, B. *et al.* Hypoxia-Induced Mesenchymal Stromal Cells Exhibit an Enhanced Therapeutic Effect on Radiation-Induced Lung Injury in Mice due to an Increased Proliferation Potential and Enhanced Antioxidant Ability. *Cell Physiol Biochem* **44**, 1295-1310, doi:10.1159/000485490 (2017).
42 Bader, A. M. *et al.* Hypoxic Preconditioning Increases Survival and Pro-Angiogenic Capacity of Human Cord Blood Mesenchymal Stromal Cells In Vitro. *PLoS One* **10**, e0138477, doi:10.1371/journal.pone.0138477 (2015).
43 Leroux, L. *et al.* Hypoxia preconditioned mesenchymal stem cells improve vascular and skeletal muscle fiber regeneration after ischemia through a Wnt4-dependent pathway. *Mol Ther* **18**, 1545-1552, doi:10.1038/mt.2010.108 (2010).
44 Lei, X. *et al.* Mesenchymal Stem Cell-Derived Extracellular Vesicles Attenuate Radiation-Induced Lung Injury via miRNA-214-3p. *Antioxid Redox Signal*, doi:10.1089/ars.2019.7965 (2020).

45 Potter, D. R. *et al.* Mesenchymal stem cell-derived extracellular vesicles attenuate pulmonary vascular permeability and lung injury induced by hemorrhagic shock and trauma. *J Trauma Acute Care Surg* **84**, 245-256, doi:10.1097/ta.0000000000001744 (2018).

46 Almiron Bonnin, D. A. *et al.* Secretion-mediated STAT3 activation promotes self-renewal of glioma stem-like cells during hypoxia. *Oncogene* **37**, 1107-1118, doi:10.1038/onc.2017.404 (2018).

47 Zhou, L. *et al.* TGF-beta-induced Foxp3 inhibits T(H)17 cell differentiation by antagonizing RORgammat function. *Nature* **453**, 236-240, doi:10.1038/nature06878 (2008).

48 Harris, T. J. *et al.* Cutting edge: An in vivo requirement for STAT3 signaling in TH17 development and TH17-dependent autoimmunity. *J Immunol* **179**, 4313-4317, doi:10.4049/jimmunol.179.7.4313 (2007).

49 Schweiger, M. W. *et al.* Extracellular Vesicles Induce Mesenchymal Transition and Therapeutic Resistance in Glioblastomas through NF-kappaB/STAT3 Signaling. *Adv Biosyst* **4**, e1900312, doi:10.1002/adbi.201900312 (2020).

50 Gaffen, S. L., Jain, R., Garg, A. V. & Cua, D. J. The IL-23-IL-17 immune axis: from mechanisms to therapeutic testing. *Nat Rev Immunol* **14**, 585-600, doi:10.1038/nri3707 (2014).

51 Thery, C. *et al.* Minimal information for studies of extracellular vesicles 2018 (MISEV2018): a position statement of the International Society for Extracellular Vesicles and update of the MISEV2014 guidelines. *J Extracell Vesicles* **7**, 1535750, doi:10.1080/20013078.2018.1535750 (2018).

52 Lotvall, J. *et al.* Minimal experimental requirements for definition of extracellular vesicles and their functions: a position statement from the International Society for Extracellular Vesicles. *J Extracell Vesicles* **3**, 26913, doi:10.3402/jev.v3.26913 (2014).

53 Glant, T. T. *et al.* Characterization and Localization of Citrullinated Proteoglycan Aggrecan in Human Articular Cartilage. *PLoS One* **11**, e0150784, doi:10.1371/journal.pone.0150784 (2016).

54 Misjak, P. *et al.* The role of citrullination of an immunodominant proteoglycan (PG) aggrecan T cell epitope in BALB/c mice with PG-induced arthritis. *Immunol Lett* **152**, 25-31, doi:10.1016/j.imlet.2013.03.005 (2013).